# Novel 5-Hydroxytryptamine (5-HT₃) Receptor Antagonists. III.[1] Pharmacological Evaluations and Molecular Modeling Studies of Optically Active 4,5,6,7-Tetrahydro-1*H*-benzimidazole Derivatives

Mitsuaki Ohta,*,[a] Takeshi Suzuki,[a] Toshio Furuya,[b] Hiroyuki Kurihara,[b] Tatsuhiro Tokunaga,[b] Keiji Miyata,[a] and Isao Yanagisawa[a]

*Neuroscience/Gastrointestinal Research Laboratories,[a] Molecular Chemistry Research Laboratories,[b] Institute for Drug Discovery Research, Yamanouchi Pharmaceutical Co., Ltd., 21 Miyukigaoka, Tsukuba, Ibaraki 305, Japan.*

The *R*- and *S*-enantiomers of the 4,5,6,7-tetrahydro-1*H*-benzimidazole derivatives **3**—**8** were prepared by optical resolution. Each *R*-isomer, except for **3**, was almost two orders of magnitude more potent than its *S*-isomer as a 5-hydroxytryptamine (5-HT₃) receptor antagonist, as judged from the effect on the von Bezold-Jarisch reflex (B. J. reflex) in rats, the contraction of isolated guinea-pig colon and the receptor-binding affinity. The (−)-(*R*)-5-[(1-methyl-1*H*-indol-3-yl)carbonyl] derivative **6***R*·HCl (ramosetron = YM060) and (−)-(*R*)-5-[(1-indolinyl)carbonyl] derivative **4***R*·HCl (YM114 = KAE-393) given *p.o.* were hundreds of times more potent than **1** (ondansetron) and **2** (granisetron) in their inhibitory effects on cisplatin-induced emesis in ferrets and restraint stress-induced increases in fecal pellet output in rats. Three-dimensional molecular modeling studies suggested that the 'chiral selection' of the enantiomers might be influenced by the steric repulsion between the aromatic ring part and the conformationally restricted 4,5,6,7-tetrahydro-1*H*-benzimidazole ring in "equatorial-twist" conformation. In our pharmacophore model for the 5-HT₃ receptor antagonist, a basic center exists at the left side of the aromatic-carbonyl plane when viewing from the aromatic part with the carbonyl oxygen atom upwards, whereas the "handedness" is ambiguous in the previously proposed model.

**Key words** YM060 (ramosetron); YM114 (KAE-393); 5-hydroxytryptamine receptor antagonist; optical resolution; three-dimensional molecular modeling

In the last decade, research on 5-hydroxytryptamine (5-HT₃) receptor antagonists has been accelerated, in view of the possible roles of these antagonists as therapeutic agents for the treatment of nausea and vomiting associated with cancer chemotherapy, pain of vascular origin, disorders of the central nervous system, and gastrointestinal disorders.[2] Among 5-HT₃ receptor antagonists, ondansetron **1**[3] and granisetron **2**[4] are already in clinical use to suppress vomiting associated with cancer chemotherapy (Chart 1).

Computer-based three-dimensional steric molecular models of the 5-HT₃ receptor pharmacophore have been developed on the basis of radio-ligand binding data using potent agents, including **1** and **2**. Regarding the chemical template and "ligand-occupied volume" of 5-HT₃ receptor antagonists, key features appear to be a carbonyl group coplanar to an aromatic ring and a basic center of appropriate position and dimensions.[5] In addition, Evans *et al.* noted that it is necessary to find novel and more selective 5-HT₃ receptor antagonists, *e.g.*, chiral ligands, to identify the pharmacophore; few studies have investigated the stereostructural requirements for 5-HT₃ receptor antagonists.[5c]

We have searched for new potent 5-HT₃ receptor antagonists which may be useful for the treatment of irritable bowel syndrome (IBS) as well as nausea and vomiting associated with cancer chemotherapy. In the preceding papers,[1] we reported a novel series of the 4,5,6,7-tetrahydro-1*H*-benzimidazole derivatives, such as **3**—**8**, to be 5-HT₃ receptor antagonists: the potency of **3** and **5** was modest, but that of **4**, **6**, **7** and **8** was very strong (Chart 1). Each of these compounds **3**—**8** is a racemate which possesses an asymmetric carbon atom at the

5-position in the 4,5,6,7-tetrahydro-1*H*-benzimidazole ring.

In this paper, we report the preparation of the enantiomers of **3**—**8** and the evaluation of their 5-HT₃ receptor antagonistic activities. The stereo selectivity of the 5-HT₃ receptor pharmacophore is also discussed based on three-dimensional molecular modeling studies.

**Chemistry**
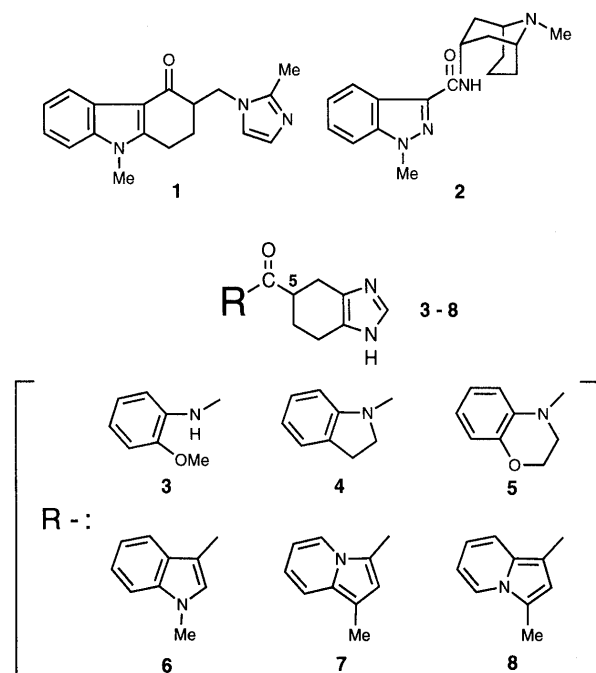
The racemates (±)-**3**—**8** were optically resolved as salts



Chart 1

with optically active dicarboxylic acids ((+)- or (−)-tartaric acid (TA), or (+)- or (−)-$O,O'$-dibenzoyltartaric acid (DIBTA)). The salts were converted to the hydrogen chloride salts to afford 3S·HCl—8S·HCl and 3R·HCl—8R·HCl, respectively (Chart 2). Analytical data for the compounds are summarized in Table 1. The optical purity was determined to be more than 99.8% in each case, based on peak area in chiral HPLC analysis.

**X-Ray Analysis** The crystallographic and experimental data for 3R·HCl, 3S·(−)-DIBTA, 4R·(+)-TA, 5R·(+)-TA and 6R·(+)-DIBTA are given in Table 2 (atomic coordinates available from Cambridge Structural Database). In the crystal structure of each compound (Chart 3), the nitrogen atom at the 3-position in the 4,5,6,7-tetrahydro-1H-benzimidazole ring is protonated and bound to the conjugate anion. The conformation of
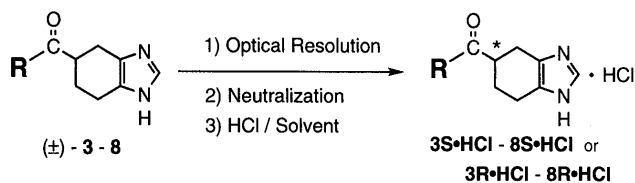


Chart 2

Table 1. Analytical Data

| Compound No. | mp (°C) (Recryst. solvent) | $[\alpha]_D^{20}$ (Solv, c) | Formula | Elemental analysis (%) Calcd (Found) C | H | N | Cl | Optical purity (area%) | Retention time (min) | Solvent system (A/B)[a] |
|---|---|---|---|---|---|---|---|---|---|---|
| 3S·(−)-DIBTA | 142.0—143.5 (DMF–H₂O) | −55.9° (DMF, 1.02) | $C_{15}H_{17}N_3O_2$·$C_{18}H_{14}O_8$·1.2H₂O | 60.86 (60.86) | 5.17 (5.17) | 6.45 (6.61) |  | >99.9 | 10.5 | 65/35 |
| 3S·HCl | 215.0—222.0 (dec.) (EtOH) | −12.2° (MeOH, 1.08) | $C_{15}H_{17}N_3O_2$·HCl·0.5H₂O | 56.87 (56.77) | 6.05 (6.01) | 13.26 (13.24) | 11.75 (11.86) | 99.8 | 10.5 | 65/35 |
| 3R·(+)-DIBTA | 139.0—141.0 (DMF–H₂O) | +56.1° (DMF, 1.03) | $C_{15}H_{17}N_3O_2$·$C_{18}H_{14}O_8$·1.1H₂O | 61.03 (60.99) | 5.15 (5.11) | 6.47 (6.57) |  | 99.8 | 12.0 | 65/35 |
| 3R·HCl | 217—223 (dec.) (EtOH) | +12.3° (MeOH, 1.09) | $C_{15}H_{17}N_3O_2$·HCl | 58.54 (58.54) | 6.01 (5.93) | 13.24 (13.59) | 11.52 (11.87) | 99.9 | 12.0 | 65/35 |
| 4S·(−)-TA | 229.5—230.5 (MeOH)[b] | −1.5° (DMF, 0.71) | $C_{16}H_{17}N_3O$·$C_4H_6O_6$ | 57.55 (57.55) | 5.55 (5.51) | 10.07 (10.08) |  | >99.9 | 14.5 | 65/35 |
| 4S·HCl | 241—244 (dec.) (EtOH–AcOEt) | +19.1° (MeOH, 1.06) | $C_{16}H_{17}N_3O$·HCl | 63.26 (63.18) | 5.97 (6.04) | 13.83 (13.78) | 11.67 (11.45) | >99.9 | 14.5 | 65/35 |
| 4R·(+)-TA | 229.0—230.0 (MeOH)[b] | +1.6° (DMF, 0.71) | $C_{16}H_{17}N_3O$·$C_4H_6O_6$ | 57.55 (57.49) | 5.55 (5.57) | 10.07 (10.06) |  | 99.9 | 17.5 | 65/35 |
| 4R·HCl | 239—242 (dec.) (EtOH–AcOEt) | −19.2° (MeOH, 1.07) | $C_{16}H_{17}N_3O$·HCl | 63.26 (63.07) | 5.97 (5.99) | 13.83 (13.76) | 11.67 (11.58) | 99.8 | 17.5 | 65/35 |
| 5S·(−)-TA | 227.0—228.0 (H₂O–MeOH)[b] | −34.2° (DMF, 1.04) | $C_{16}H_{17}N_3O_2$·$C_4H_6O_6$ | 55.42 (55.24) | 5.35 (5.21) | 9.70 (9.60) |  | >99.9 | 13.0 | 50/50 |
| 5S·HCl | 189.0—190.0 (EtOH–AcOEt) | −12.3° (MeOH, 1.02) | $C_{16}H_{17}N_3O_2$·HCl·0.15H₂O | 59.59 (59.63) | 5.72 (5.64) | 13.03 (13.06) | 10.99 (11.32) | >99.9 | 13.0 | 50/50 |
| 5R·(+)-TA | 227.0—228.0 (H₂O–MeOH)[b] | +34.6° (DMF, 1.05) | $C_{16}H_{17}N_3O_2$·$C_4H_6O_6$ | 55.42 (55.18) | 5.35 (5.28) | 9.70 (9.70) |  | 99.8 | 15.5 | 50/50 |
| 5R·HCl | 188.0—189.0 (EtOH–AcOEt) | +12.3° (MeOH, 1.10) | $C_{16}H_{17}N_3O_2$·HCl·0.15H₂O | 59.59 (59.52) | 5.72 (5.67) | 13.03 (13.01) | 10.99 (11.10) | 99.8 | 15.5 | 50/50 |
| 6S·(−)-DIBTA | 168.5—169.5 (DMF–H₂O) | −30.3° (DMF, 1.07) | $C_{17}H_{17}N_3O$·$C_{18}H_{14}O_8$·H₂O | 64.12 (64.13) | 5.07 (5.13) | 6.41 (6.71) |  | 99.9 | 13.5 | 50/50 |
| 6S·HCl | 230—234 (dec.) (EtOH–AcOEt) | +42.9° (MeOH, 1.12) | $C_{17}H_{17}N_3O$·HCl | 64.66 (64.47) | 5.75 (5.76) | 13.31 (13.15) | 11.23 (11.21) | 99.9 | 13.5 | 50/50 |
| 6R·(+)-DIBTA | 169.0—170.0 (DMF–H₂O) | +30.6° (DMF, 1.10) | $C_{17}H_{17}N_3O$·$C_{18}H_{14}O_8$·H₂O | 64.12 (64.13) | 5.07 (5.13) | 6.41 (6.55) |  | 99.9 | 16.5 | 50/50 |
| 6R·HCl | 215—230 (dec.) (EtOH–AcOEt) | −42.9° (MeOH, 1.02) | $C_{17}H_{17}N_3O$·HCl | 64.66 (64.37) | 5.75 (5.80) | 13.31 (13.12) | 11.23 (11.17) | 99.8 | 16.5 | 50/50 |
| 7S·(+)-DIBTA | 139.0—139.5 (DMF–H₂O) | +51.8° (DMF, 1.77) | $C_{17}H_{17}N_3O$·$C_{18}H_{14}O_8$·1.5DMF[c]·H₂O | 62.00 (62.21) | 5.73 (5.62) | 8.24 (8.41) |  | >99.9 | 13.5 | 30/70 |
| 7S·HCl | 238—241 (dec.) (EtOH–AcOEt) | +8.2° (MeOH, 1.13) | $C_{17}H_{17}N_3O$·HCl | 64.66 (64.52) | 5.75 (5.75) | 13.31 (13.27) | 11.23 (11.26) | 99.9 | 13.5 | 30/70 |
| 7R·(−)-DIBTA | 138.0—138.5 (DMF–H₂O) | −51.8° (DMF, 1.88) | $C_{17}H_{17}N_3O$·$C_{18}H_{14}O_8$·1.5DMF[c]·H₂O | 62.00 (62.09) | 5.73 (5.55) | 8.24 (8.35) |  | 99.9 | 16.0 | 30/70 |
| 7R·HCl | 236—239 (dec.) (EtOH–AcOEt) | −8.5° (MeOH, 1.14) | $C_{17}H_{17}N_3O$·HCl | 64.66 (64.55) | 5.75 (5.75) | 13.31 (13.24) | 11.23 (11.32) | 99.8 | 16.0 | 30/70 |
| 8S·(+)-DIBTA | 145.5—146.0 (DMF–H₂O) | +38.9° (DMF, 1.09) | $C_{17}H_{17}N_3O$·$C_{18}H_{14}O_8$·0.5H₂O | 65.01 (64.86) | 4.99 (4.93) | 6.50 (6.41) |  | >99.9 | 12.5 | 30/70 |
| 8S·HCl | 237—240 (dec.) (EtOH–AcOEt) | +15.7° (MeOH, 1.13) | $C_{17}H_{17}N_3O$·HCl·0.5H₂O | 62.86 (62.71) | 5.90 (5.88) | 12.94 (12.80) | 10.91 (11.18) | >99.9 | 12.5 | 30/70 |
| 8R·(+)-DIBTA | 166.5—167.0 (DMF–H₂O) | +39.5° (DMF, 1.04) | $C_{17}H_{17}N_3O$·$C_{18}H_{14}O_8$·1.5DMF[c]·H₂O | 62.00 (61.98) | 5.73 (5.60) | 8.24 (8.54) |  | >99.9 | 13.5 | 30/70 |
| 8R·HCl | 238—242 (dec.) (EtOH–AcOEt) | −15.9° (MeOH, 1.11) | $C_{17}H_{17}N_3O$·HCl·0.2H₂O | 63.93 (63.96) | 5.81 (5.83) | 13.16 (13.01) | 11.10 (11.36) | >99.9 | 13.5 | 30/70 |

a) A=0.05 M $Na_2HPO_4$–$H_3PO_4$ (pH 5.2) and B=$CH_3CN$.  b) See experimental section.  c) Dimethylformamide=$C_3H_7NO$.

Table 2. Crystallographic and Experimental Data

| | 3S·(−)-DIBTA | 3R·HCl | 4R·(+)-TA | 5R·(+)-TA | 6R·(+)-DIBTA |
|---|---|---|---|---|---|
| Mol. formula | $C_{33}H_{33}N_3O_{11}$ | $C_{15}H_{18}ClN_3O_2$ | $C_{20}H_{23}N_3O_7$ | $C_{20}H_{23}N_3O_8$ | $C_{35}H_{33}N_3O_{10}$ |
| $M_r$ | 647.64 | 307.78 | 417.42 | 433.42 | 655.66 |
| Space group | $P2_1$ | $P2_12_12_1$ | $P2_12_12_1$ | $P2_12_12_1$ | $P2_1$ |
| $a$, Å | 22.230 (7) | 7.237 (2) | 9.259 (2) | 9.263 (3) | 22.042 (4) |
| $b$, Å | 9.528 (2) | 32.513 (2) | 29.68 (1) | 29.15 (4) | 9.571 (1) |
| $c$, Å | 7.517 (1) | 7.057 (3) | 7.601 (4) | 7.615 (4) | 7.545 (2) |
| $\beta$, deg | 95.75 (3) | | | | 95.30 (3) |
| $V$, Å³ | 1584.1 (6) | 1660.5 (6) | 2089 (1) | 2056 (1) | 1584.9 (5) |
| $Z$ | 2 | 4 | 4 | 4 | 2 |
| $D_{calc}$, g/cm³ | 1.358 | 1.231 | 1.317 | 1.400 | 1.374 |
| No. of unique reflcns | 1976 | 1411 | 2477 | 1680 | 2460 |
| No. of reflcns used | 1916 | 1321 | 2230 | 1460 | 2347 |
| $R$ | 4.80 | 6.43 | 3.93 | 4.56 | 4.87 |
| $R_w$ | 4.87 | 7.11 | 3.74 | 4.45 | 4.94 |
| Max shift non-H | 0.314 | 0.156 | 0.205 | 0.049 | 0.147 |



**3R•HCl**

**3S•(-)-DIBTA**

**4R•(+)-TA**

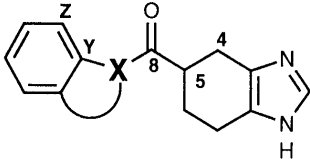**5R•(+)-TA**

**6R•(+)-DIBTA**

Chart 3
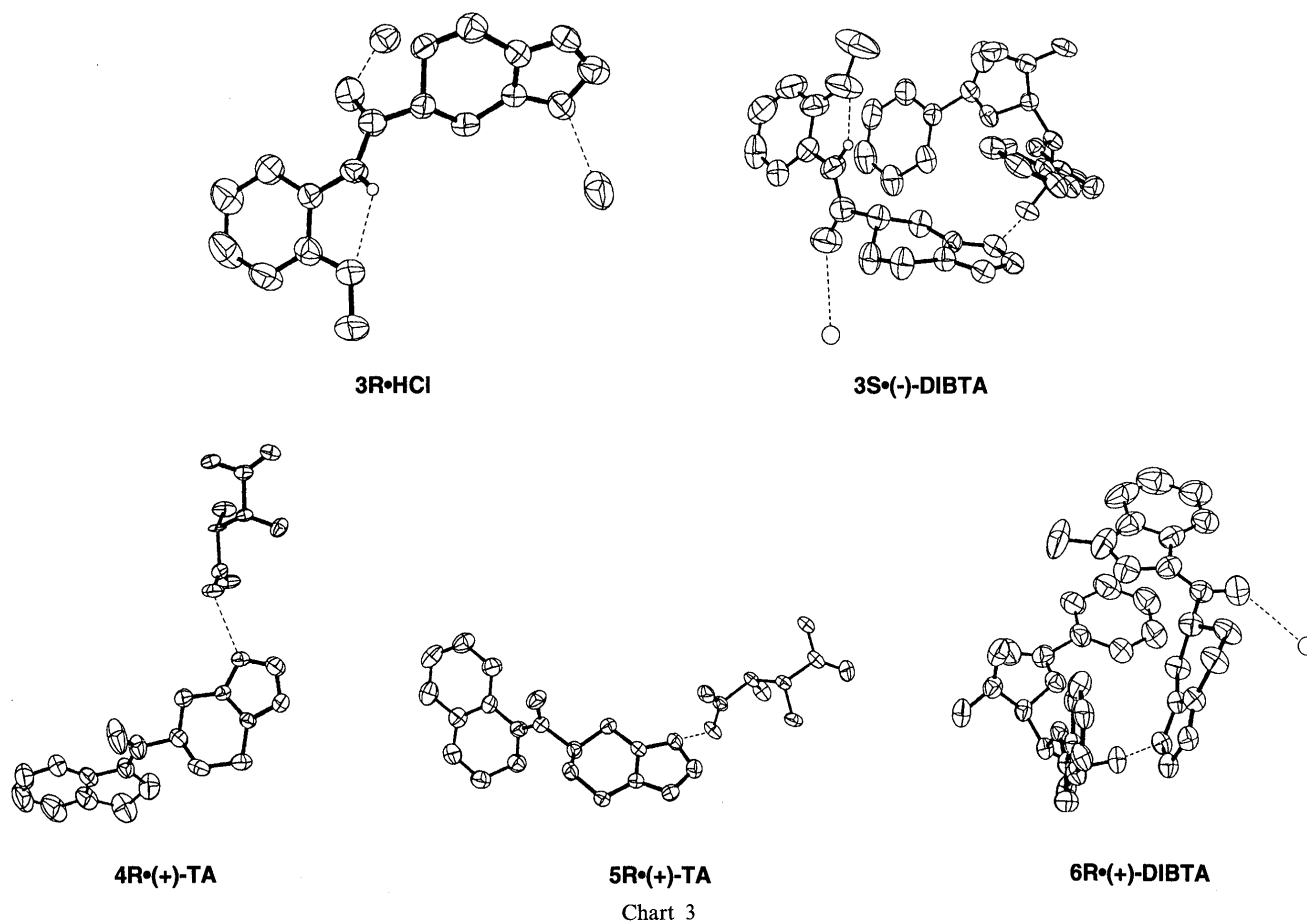
3R·HCl was nearly identical with that of the enantiomorph of 3S·(−)-DIBTA, in spite of differences in crystal packing and the kind of bound salt. There was an intramolecular hydrogen bond between the methoxy oxygen atom on the benzene ring and the amide hydrogen atom in both 3R·HCl and 3S·(−)-DIBTA, forming a pseudo 6–5 fused ring with the benzene ring. The carbonyl group was located in almost the same plane as the benzene ring due to the presence of this hydrogen bond. The coplanar relationship between the aromatic ring and carbonyl group was also observed in other compounds, except for 5R·(+)-TA, which does not possess a flat conformation of its benzoxazine-carbonyl part.
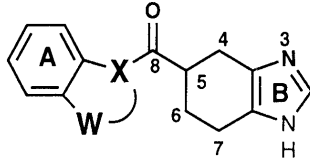


Chart 4
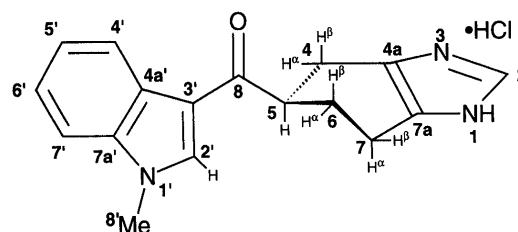
As for the 4,5,6,7-tetrahydrobenzimidazole ring moiety, the conformations in four R-enantiomers, 3R·HCl, 4R·(+)-TA, 5R·(+)-TA and 6R·(+)-DIBTA, were quite

Table 3. Selected Torsion Angles (deg)



| | 3S·(−)-DIBTA | 3R·HCl | 4R·(+)-TA | 5R·(+)-TA | 6R·(+)-DIBTA |
|---|---|---|---|---|---|
| $\tau^1$ $(C^Z-C^Y-X-C^8)$ | 20.8 | −27.8 | 0.4 | 37.8 | −3.5 |
| $\tau^2$ $(C^Y-X-C^8-O)$ | −8.3 | 5.1 | 6.7 | 3.9 | −0.7 |
| $\tau^{2'}$ $(C^Y-X-C^8-C^5)$ | 169.1 | −173.9 | −173.8 | −174.3 | −174.7 |
| $\tau^3$ $(O-C^8-C^5-C^4)$ | 80.3 | −88.0 | −35.7 | −56.4 | −89.5 |
| $\tau^{3'}$ $(X-C^8-C^5-C^4)$ | −97.2 | 90.9 | 144.8 | 121.8 | 84.7 |
| $\tau^1+\tau^2$ | 12.5 | −22.7 | 7.1 | 41.7 | −4.2 |

Table 4. Comparision of Geometrical Parameters



| | Deviation of plane A (Å) | | | | | | Deviation of plane B (Å) | | | | Plane A/B (deg) | A*–N* (Å) | O–N* (Å) |
|---|---|---|---|---|---|---|---|---|---|---|---|---|---|
| | X | W | $C^8$ | O | $C^5$ | N* | $C^4$ | $C^5$ | $C^6$ | $C^7$ | | | |
| 3S·(−)-DIBTA | 0.07 | −0.01 | 0.51 | 0.80 | 0.70 | 3.04 | −0.02 | −0.34 | 0.49 | 0.05 | 114.8 | 8.8 | 5.9 |
| 3R·HCl | 0.05 | 0.05 | −0.39 | −0.81 | −0.35 | −2.35 | 0.01 | 0.24 | −0.51 | 0.04 | 125.5 | 8.9 | 6.0 |
| 4R·(+)-TA | −0.05 | 0.06 | −0.09 | 0.03 | −0.29 | −1.25 | 0.02 | 0.44 | −0.32 | 0.01 | 126.6 | 9.1 | 5.8 |
| 5R·(+)-TA | −0.04 | −0.03 | 0.61 | 1.32 | 0.43 | 0.16 | 0.05 | 0.51 | −0.22 | 0.02 | 138.0 | 9.0 | 5.8 |
| 6R·(+)-DIBTA | −0.06 | −0.04 | −0.19 | −0.29 | −0.36 | −2.60 | 0.02 | 0.52 | −0.24 | 0.04 | 111.6 | 9.1 | 6.0 |

A*; center of the benzene ring A. N*; centroid of $N^3-C^2-N^1$ in the imidazole ring.

similar to each other. In this moiety, the cyclohexene ring part takes "twist" conformation with the carbonyl group at the "5-equatorial" position (see Chart 4). This "equatorial-twist" conformation may minimize steric repulsion between the cyclohexene ring and the neighboring fused bicyclic ring. The "equatorial-twist" conformation was also expected in the aqueous solution, based on NMR studies of 6R·HCl described below.

Selected torsion angles and geometrical parameters for 3R·HCl, 3S·(−)-DIBTA, 4R·(+)-TA, 5R·(+)-TA and 6R·(+)-DIBTA are listed in Tables 3 and 4.

**Determination of Absolute Configuration** Absolute configuration at the 5-position of the 4,5,6,7-tetrahydro-1H-benzimidazole ring in each 3S·(−)-DIBTA, 4R·(+)-TA, 5R·(+)-TA and 6R·(+)-DIBTA was determined to be S, R, R and R, respectively, based on the known absolute stereochemistries of (−)- and (+)-DIBTA, and (+)-TA (Chart 3). Since we have not obtained crystals of 7R, 7S, 8R or 8S, their absolute configurations were deduced from chiral HPLC analysis, where the retention time for each R-isomer seems to be longer than that for the corresponding S-isomer (Table 1).

**NMR Studies** We have reported that the 6–5 fused (or pseudo-fused) ring and the carbonyl group in 3, 4, 6, 7 and 8 are in the same plane, but this is not the case in 5, which has a 6–6 fused ring, based on a $^1$H-NMR study.[1b] Detailed NMR studies (in $D_2O$) were performed to de-

termine the conformation of 6R·HCl. Examination of the 1-D ($^1$H- and $^{13}$C-NMR) and 2-D (correlation spectroscopies (COSY), heteronuclear multiple-bond correlation (HMBC) and heteronuclear single-quantum coherence (HSQC)) spectral data for 6R·HCl allowed a complete and unambiguous assignment of all protons and carbons (Table 5; see Chart 4 for numbering): observed coupling constants and nuclear Overhauser effect (NOE) data obtained by rotating-frame Overhauser enhancement spectroscopy (ROESY) for the protons at the cyclohexene ring of the 4,5,6,7-tetrahydro-1H-benzimidazole moiety are summarized in Table 6.

Coupling constants between $H^5$ and $H^{4\alpha}$, $H^{4\beta}$, $H^{6\alpha}$ and $H^{6\beta}$ were 5.5, 9.3, 2.7 and 10.7 Hz, respectively. These results suggest that both $H^{4\beta}$ and $H^{6\beta}$ exist at the anti-periplanar position to $H^5$, and that $H^{4\beta}$, $H^5$ and $H^{6\beta}$ are each at the axial or pseudo-axial position. In addition, NOE between $H^5$ and each of $H^{2'}$, $H^{4\alpha}$ or $H^{6\alpha}$ was observed. These observations demonstrate that, in $D_2O$, the cyclohexene ring part in the 4,5,6,7-tetrahydro-1H-benzimidazole moiety of 6R·HCl may adopt the twist conformation, and that the indole-carbonyl moiety may be located at the 5β (equatorial) position (Chart 4).

**Pharmacological Results**

Each enantiomer of 3—8 was evaluated for 5-HT$_3$ receptor antagonistic activity (Table 7). Data are present-

Table 5. NMR Assignment for 6R·HCl

| Numbering[a] | $\delta$ ($^1$H-NMR)[b] | $\delta$ ($^{13}$C-NMR)[b] |
|---|---|---|
| 2 | 8.47 (s) | 134.3 |
| 4a | — | 129.1 |
| 4 | | 25.2 |
| $\alpha$ | 2.70 (dd) | |
| $\beta$ | 2.82 (dd) | |
| 5 | 3.46 (m) | 44.9 |
| 6 | | 29.4 |
| $\alpha$ | 2.16 (m) | |
| $\beta$ | 1.80 (m) | |
| 7 | | 22.0 |
| $\alpha$ | 2.66 (m) | |
| $\beta$ | 2.72 (m) | |
| 7a | — | 129.5 |
| 8 | — | 202.3 |
| 2' | 8.09 (s) | 142.0 |
| 3' | — | 116.2 |
| 4'a | — | 128.5 |
| 4' | 8.12 (d) | 124.0 |
| 5' | 7.33 (dd) | 126.0 |
| 6' | 7.37 (dd) | 126.6 |
| 7' | 7.44 (dd) | 113.6 |
| 7'a | — | 140.4 |
| 8' | 3.81 (s) | 36.0 |

a) See Chart 4. b) Sodium ($\beta$-trimethylsilyl)propionate was used as a reference in $D_2O$.

Table 6. Observed Coupling Constants and NOE for 6R·HCl

| Coupling constant (Hz) | | NOE |
|---|---|---|
| $J_{4\alpha,4\beta} = 16.0$ | $J_{6\alpha,7\alpha} = 4.6$ | $H^{4\alpha} \leftrightarrow H^{4\beta}$ |
| $J_{6\alpha,6\beta} = 13.4$ | $J_{6\alpha,7\beta} = 4.6$ | $H^{6\alpha} \leftrightarrow H^{6\beta}$ |
| $J_{7\alpha,7\beta} = 16.5$ | $J_{6\beta,7\alpha} = 9.8$ | $H^{7\alpha} \leftrightarrow H^{7\beta}$ |
| $J_{5,4\beta} = 9.3$ | $J_{6\beta,7\beta} = 5.9$ | $H^{4\alpha} \leftrightarrow H^5$ |
| $J_{5,4\alpha} = 5.5$ | | $H^{6\alpha} \leftrightarrow H^5$ |
| $J_{5,6\beta} = 10.7$ | | $H^{2'} \leftrightarrow H^5$ |
| $J_{5,4\alpha} = 2.7$ | | |

ed as the $ID_{50}$ values (nmol/kg, i.v.) against the von Bezold-Jarisch reflex (B. J. reflex)[6] induced by 5-HT (170 nmol/kg, i.v.) in rats and the $IC_{50}$ values ($\mu$M) against the contractile responses to 5-HT (50 $\mu$M) in isolated guinea-pig distal colon.[7]

Every $R$-isomer was found to be a more potent antagonist than the corresponding $S$-isomer on the B. J. reflex. The $R$- to $S$-isomer potency ratios were 20, over 100, 700, 220, 95 and 270 for 3, 4, 5, 6, 7, and 8, respectively. Among the $R$-isomers, 8R·HCl showed great potency ($ID_{50} = 0.024$ nmol/kg), being about 270 and 88 times more potent than 1 and 2, respectively. In terms of the effect on colonic contraction, every $R$-isomer was also more potent than the corresponding $S$-isomer, except for 3, which showed similar potency of the enantiomers. The $R$- to $S$-isomer potency ratios were 160, 43, 180, 20 and 58 for 4, 5, 6, 7 and 8, respectively. Among them, 6R·HCl exhibited strong activity ($IC_{50} = 0.012$ $\mu$M), being about 65 and 5 times more potent than 1 and 2, respectively. Although the activity of 4R·HCl or 5R·HCl was rather weak on the B. J. reflex, both had potent effects on the colonic contraction. A similar observation was made for the racemates.[1b] Further, the non-5-HT$_3$ receptor-blocking activities of 4R·HCl, 6R·HCl, 7R·HCl and

Table 7. 5-HT$_3$ Receptor-Antagonistic Activities and Binding Affinity

| Compd. No. | 5-HT$_3$ receptor-antagonistic activities | | $K_i$ (nM) for 5-HT$_3$ receptor binding |
|---|---|---|---|
| | $ID_{50}$ (nmol/kg i.v.) on B.J. reflex | $IC_{50}$ ($\mu$M) of colon contraction | |
| 3S·HCl | 30 | 1.6 | NT |
| | [20—44][a] | [0.90—3.0] | |
| 3R·HCl | 1.5 | 3.9 | NT |
| | [0.77—3.0] | [2.8—5.4] | |
| 4S·HCl | (9%)[b] | 4.1 | 620 |
| | | [2.6—6.4] | [590—640] |
| 4R·HCl | 1.1 | 0.026 | 0.34 |
| | [0.95—1.3] | [0.0070—0.096] | [0.33—0.35] |
| 5S·HCl | 11000 | 6.0 | NT |
| | [6000—20000] | [4.8—7.5] | |
| 5R·HCl | 15 | 0.14 | NT |
| | [9.4—25] | [0.070—0.30] | |
| 6S·HCl | 29 | 2.2 | 10.3 |
| | [24—33] | [1.9—2.5] | [10.0—10.6] |
| 6R·HCl | 0.13 | 0.012 | 0.091 |
| | [0.11—0.15] | [0.0050—0.028] | [0.086—0.097] |
| 7S·HCl | 6.8 | 0.95 | 14.8 |
| | [3.1—15] | [0.65—1.5] | [14.4—15.3] |
| 7R·HCl | 0.072 | 0.050 | 0.092 |
| | [0.065—0.086] | [0.017—0.14] | [0.090—0.095] |
| 8S·HCl | 6.5 | 2.8 | 14.6 |
| | [4.7—9.3] | [2.3—3.3] | [14.3—14.9] |
| 8R·HCl | 0.024 | 0.048 | 0.065 |
| | [0.014—0.043] | [0.017—0.14] | [0.061—0.068] |
| 1 | 6.5 | 0.78 | 7.0 |
| | [5.1—8.6] | [0.43—1.4] | [6.0—8.1] |
| 2 | 2.1 | 0.061 | 2.0 |
| | [1.3—3.2] | [0.051—0.075] | [1.7—2.3] |

a) 95% confidence limits. b) Percent inhibition by 106 nmol/kg of drug. NT: not tested.

8R·HCl were very low (pA$_2$ < 5.0, $\leq$5.6, $\leq$5.7 and $\leq$5.5, respectively) for 5-HT$_1$-like, 5-HT$_2$, $\alpha_1$, $\alpha_2$, $\beta_1$, $\beta_2$, H$_1$ and H$_2$ receptors in *in vitro* studies.[7]

We next examined the 5-HT$_3$ receptor-binding affinity of the single isomers of 4, 6, 7 and 8. The $K_i$ values (nM) versus [$^3$H]GR65630[8] on N1E-115 cell membranes[9] are shown (Table 7). Every $R$-isomer showed a higher affinity than its corresponding $S$-isomer: the $R$- to $S$-isomer affinity ratios were 1800, 110, 160 and 220 for 4, 6, 7 and 8, respectively. In addition, $K_i$ values of over 1000 nM for 4R·HCl and 6R·HCl were found for various other receptors (5-HT$_{1A}$, 5-HT$_2$, $\alpha_1$, $\alpha_2$, D$_2$, M$_2$, $\mu$-opioid, BZP and H$_1$ receptors).[10]

These results on the antagonistic activities and the binding affinity revealed 4R·HCl, 6R·HCl, 7R·HCl and 8R·HCl to be highly potent and selective 5-HT$_3$ receptor antagonists.

**Three-Dimensional Molecular Modeling Study** Several conformational analysis studies have investigated the possible spatial relationships among three functionally important elements, an aromatic ring system, a coplanar carbonyl group and a basic center, in a large number of 5-HT$_3$ receptor antagonists,[5] and several pharmacophore models for 5-HT$_3$ receptor antagonists have been proposed. Among our 4,5,6,7-tetrahydrobenzimidazole derivatives, the $R$-isomers of certain compounds are almost two orders of magnitude more potent than their $S$-isomers. These differences in the potency are much larger

3R                           3R
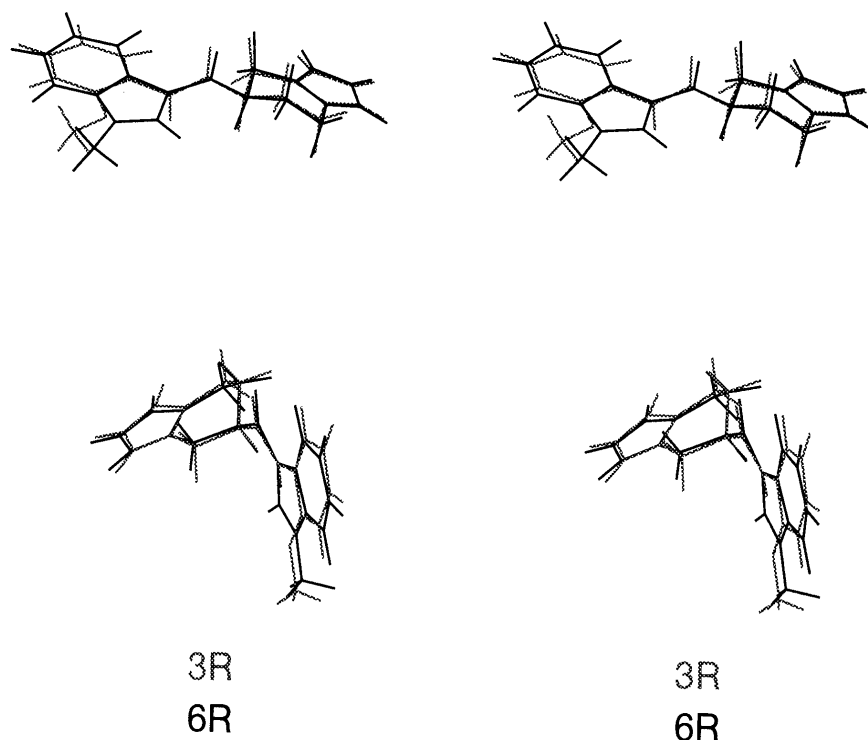6R                           6R

Chart 5.  Superimposition of Crystal Structure of **3R** (Gray) and **6R** (Black) from Different Viewpoints (Stereo Pairs)

than those for the compounds previously reported. Thus, it was expected that detailed examination of the structural features of the 4,5,6,7-tetrahydrobenzimidazole derivatives would provide useful information on "chirality selection" in the recognition site and assist the development of the pharmacophore model.

We have solved the crystal structures of four *R*-isomers, **3R**, **4R**, **5R** and **6R** (Tables 3, 4). A root-mean-square (RMS) fit was carried out using the centroid of the benzene ring (A*), the end point of the vector normal to the plane of the benzene ring from the centroid (1 Å length), the carbonyl carbon ($C^8$) and oxygen (O), and the centroid of $N^1$–$C^2$–$N^3$ in the imidazole (N*). The conformations of the four compounds are basically similar, suggesting that they are stable enough not to be greatly affected by salt binding and crystal packing force. The conformations of **3R** and **6R** are essentially the same, with RMS deviations of 0.16 Å for the 5 points described above (Chart 5). Our NMR studies indicate that the conformation of **6R** in the crystalline environment is retained in the aqueous solution.

From the results of our X-ray and NMR analysis, we attempted to predict the active conformation of the compounds. Our experimental data together with previous conformational analysis studies[5b,c] show that the carbonyl group exists in the same plane as the adjacent aromatic ring part. The potency of **5R**, in which the geometry of the oxazine ring prevents the carbonyl group from being coplanar with the aromatic ring ($\tau^1 + \tau^2$ in Table 3), is weaker than those of the other compounds examined in this study. Transoid formation for $C^Y$–X–$C^8$–$C^5$ seems to be favored, as a torsion angle ($\tau^{2'}$) of about 180° was observed (Table 3) due to the repulsion between hydrogen atoms at the Z-position in the benzene ring and at the 4,5 or 6 position in the 4,5,6,7-tetrahydrobenzimidazole ring. In addition, we hypothesized an "equatorial-twist"
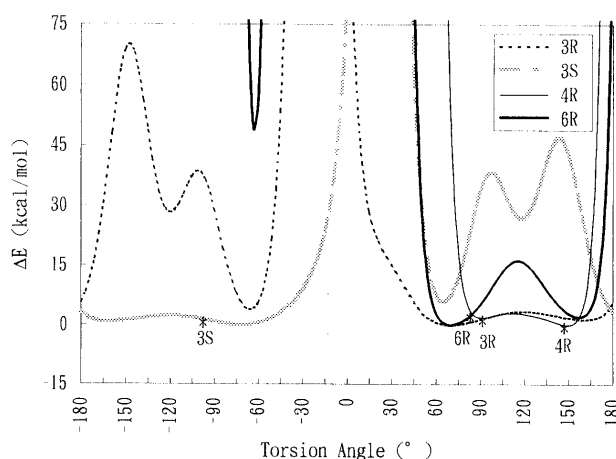


Chart 6.  Plots of van der Waals Energy Differences ($\Delta E$) from the Lowest One as a Function of the Torsion Angle X–$C^8$–$C^5$–$C^4$ for Compounds **3R**, **3S**, **4R** and **6R**

The values observed in crystal structures are presented as stars.

bioactive conformation for cyclohexene ring moiety, since this is one of the most stable conformations for the ring and was observed in all the crystal structures examined here and in the aqueous solution of **6R**.

In this series of compounds, there is a rotatable bond, $C^8$–$C^5$, whose torsion angle is represented as $\tau^{3'}$ (or $\tau^3$) in Table 3. Actually, $|\tau^{3'}|$ values range from 84.7° to 144.8° in the crystal structures, revealing the flexibility of the $C^8$–$C^5$ bond. In order to search available active conformers based on our hypothesis, we have carried out simple conformational analysis studies by rotating the $C^8$–$C^5$ bond with a step of 3° using the crystal structures of **3R**, **3S**, **4R** and **6R** (Chart 6). The calculations were performed using the SYBYL Molecular Modeling Software,[11] running on a Silicon Graphics IRIS work-
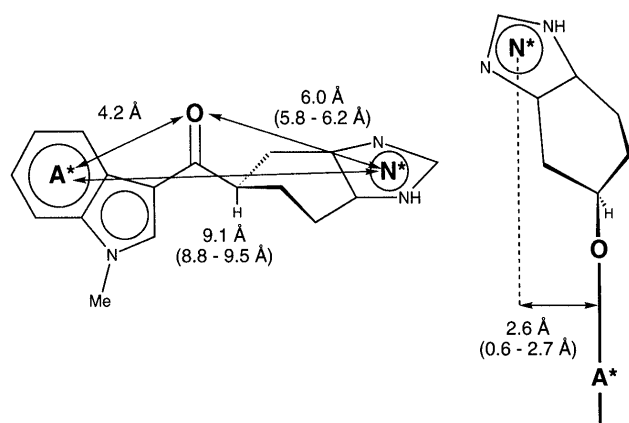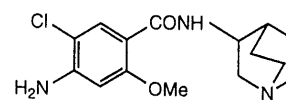
Chart 7. The Basic Pharmacophore Model for 5-HT$_3$ Receptor Antagonists Predicted from Conformational Analysis Studies Using the Crystal Structure of 6R

The interatomic distance among A*, O and N* of 6R and the ranges (in parenthesis) for energetically accepted conformers of 6R are shown in the left figure. The height of N* above the indole-carbonyl plane is also shown in the right figure.



Zacopride

Chart 8

Table 8. Inhibitory Effects on Cisplatin-Induced Emesis and Stress-Induced Defecation

| Compd. No. | ID$_{50}$ ($\mu$g/kg) on cisplatin-induced emesis | | ID$_{50}$ ($\mu$g/kg) on stress-induced defecation | |
|---|---|---|---|---|
| | i.v. | p.o. | i.v. | p.o. |
| 4R·HCl | 0.46 [0.42—0.49]$^{a)}$ | 0.65 [0.61—0.70] | 7.0 [2.8—17] | 6.9 [0.9—55] |
| 6R·HCl | 0.06 [0.05—0.07] | 0.10 [0.09—0.11] | 2.3 [1.6—3.4] | 1.1 [0.2—6.6] |
| 1 | 18 [14—24] | 50 [42—60] | 41 [18—94] | 480 [340—691] |
| 2 | 1.3 [0.8—2.3] | 44 [25—79] | 82 [46—146] | 210 [110—390] |

a) 95% confidence limits.

station. Conformers within 15 kcal/mol of the lowest-energy conformer were selected for each compound. Electrostatic energies were not included in the calculations because it is very difficult to estimate the electrostatic interaction energies with the receptor molecule. The plots of the calculated energies and the torsion angles ($\tau^{3'}$) show that energetically allowed angle is restricted to the positive value range for 4R and 6R (Chart 6). This is because of the steric repulsion between the aromatic ring and the 4,5,6,7-tetrahydrobenzimidazole moiety. Using 36 accepted conformers of 6R, a simple putative pharmacophore model is presented based on the distances between functionally important groups (Chart 7). Distance ranges from a basic center (N*; the centroid of the N–C–N atoms in the imidazole) to the centroid of the benzene ring (A*) and to the carbonyl oxygen atom are 8.8—9.5 Å (average 9.2 Å) and 5.8—6.2 Å (average 5.9 Å), respectively. (If we use the centroid of the pyrrole ring instead of that of the benzene ring in the indole moiety, the corresponding range is 6.9—7.7 Å.) The height of the basic center above the aromatic plane ranges from 0.6 to 2.7 Å. The value is larger than 2.0 Å in more than half of the accepted conformers, including the crystal structure (average 2.0 Å). This suggests that the basic center should lie away from the plane of the aromatic ring in a certain direction for stronger activity, rather than being in the plane. The distance ranges in our pharmacophore model are basically consistent with those in the previous models proposed by Hibert et al.[5b] and Evans et al.[5c]

As Evans et al.[5c] pointed out, however, there are two possibilities for the "handedness" of their model. This ambiguity could be removed by examining our pharmacophore model. In our model, it is clear that the basic center exists at the left side of the aromatic–carbonyl plane when viewing from the indole ring with the carbonyl oxygen atom upwards (Charts 5, 7).

The differences in potency between R-isomers and S-isomers may be explained in terms of the "chirality" in the arrangement of three important groups. In Chart 6, it is of interest to see that 3R has a comparatively low,

shallow and broad energy minima in the negative torsion angle range for $\tau^{3'}$, in contrast to the other R-enantiomers which have very deep and narrow ones. This is because 3R does not have a five-membered ring fused with the benzene ring. Similarly, from the energy calculations, 3S is able to take a conformation with a positive $\tau^{3'}$ value, although it is $-97.2°$ in the crystal structure (Table 3). For example, when $\tau^{3'}$ in 3S is changed to the energetically allowed value of 66°, its basic center moves to the other side of the plane of the aromatic ring with a height from it of 0.74 Å. In this case, the location of the basic center in 3S could be close to that of 3R. It seems that it is energetically difficult for other S-enantiomers to have a positive $\tau^{3'}$ torsion angle and to satisfy the required arrangement of the three groups. This is probably the reason why the potency ratio between 3R and 3S is relatively small, whereas the ratios for the others, such as 6R and 6S, are large. This consideration may be applied to other 5-HT$_3$ receptor antagonists. For instance, the affinity of (S)-zacopride is at least 8 times stronger than that of (R)-zacopride[12] (Chart 8). With the rotation of the bond connecting the bicyclo ring to the amide group, the basic nitrogen atom is able to move to both sides of the plane of the aromatic ring. Similarly, in the case of the two enantiomers of ondansetron, which were reported to be approximately equipotent,[13] the basic center could be positioned on either side of the plane by adjusting the rotatable bonds between the carbazolone ring and the imidazole ring.

**Further Pharmacological Evaluation** Compounds 4R·HCl and 6R·HCl were selected for further development among the 4,5,6,7-tetrahydro-1H-benzimidazole derivatives, based on the results of the physicochemical, pharmacokinetic and toxicologic evaluations.

Both compounds were shown to be highly potent inhibitors of cisplatin-induced emesis in ferrets[14] and restraint stress-induced increases in fecal pellet output in rats, in which endogenous 5-HT may mediate stress-

induced changes in bowel function through the 5-HT$_3$ receptor.[15] Data are presented as the ID$_{50}$ values ($\mu$g/kg) for i.v. and p.o. administration (Table 8). Compounds **4R·HCl** and **6R·HCl** given p.o., as well as i.v., potently inhibited cisplatin (10 mg/kg, i.p.)-induced emesis, with ID$_{50}$ values of 0.66 and 0.10 $\mu$g/kg, respectively (50 and 41 $\mu$g/kg for **1** and **2**, respectively). Also, p.o. doses of both compounds potently inhibited stress-induced defecation, with ID$_{50}$ values of 6.9 and 1.1 $\mu$g/kg, respectively (480 and 210 $\mu$g/kg for **1** and **2**, respectively). The p.o.-to-i.v. ID$_{50}$ ratios for emesis and defecation were 1.5 and 1 for **4R·HCl**, 2 and 0.5 for **6R·HCl**, 3 and 20 for **1**, and 30 and 2.5 for **2**, respectively. These results may suggest higher bioavailability of **4R·HCl** and **6R·HCl** than of **1** and **2**.

In these two experiments, a greater difference in inhibitory effects between **4R·HCl** or **6R·HCl** and **1** or **2** was found in comparison with that for the 5-HT$_3$ receptor-antagonistic activities (Tables 7, 8). This observation might be explained on the basis of duration of action. The inhibitory effect of single doses (i.v. and p.o.) of **4R·HCl** and **6R·HCl** on the von B. J. reflex lasted as long as that of **2** and longer than that of **1**. Further, in vitro 5-HT$_3$ receptor antagonistic-activity of **4R·HCl** and **6R·HCl** in the 5-HT-induced colonic contraction model persisted significantly longer than that of **1** and **2** after washout of the compounds.[16]

Compounds **6R·HCl** (ramosetron = YM060) and **4R·HCl** (YM114 = KAE-393) are currently under clinical trial for the treatment of IBS as well as nausea and vomiting associated with cancer chemotherapy.

## Conclusion

The R- and S-enantiomers of the 4,5,6,7-tetrahydro-1H-benzimidazole derivatives **3**—**8** were prepared by optical resolution, and, except for **3**, each R-isomer was found to be almost by two orders of magnitude more potent than its S-isomer as a 5-HT$_3$ receptor antagonist in terms of effect on the B. J. reflex in rats, contraction of isolated guinea-pig colon and receptor binding affinity.

Three-dimensional molecular modeling studies suggested that "chiral selection" might be related to the steric repulsion between the aromatic ring part and the conformationally restricted 4,5,6,7-tetrahydro-1H-benzimidazole ring in "equatorial-twist" conformation. In our pharmacophore model for the 5-HT$_3$ receptor antagonist, the basic center exists at the left side of the aromatic–carbonyl plane when viewing from the indole ring with the carbonyl oxygen atom upwards, whereas the "handedness" remained ambiguous in the previously proposed model.

The selected compounds **6R·HCl** (ramosetron = YM060) and **4R·HCl** (YM114 = KAE-393) were found to be highly potent inhibitors of cisplatin-induced emesis in ferrets and restraint stress-induced increase in fecal pellet output in rats, and to be several hundred times more potent than **1** and **2** on p.o. administration in these experiments. Both compounds are currently under clinical trial for the treatment of IBS, as well as nausea and vomiting associated with cancer chemotherapy.

## Experimental

All melting points were determined on a Yanaco MP-500D melting point apparatus and are uncorrected. NMR spectra were measured with a JEOL JNM-A500 FT NMR spectrometer. Chemical shifts are recorded in $\delta$ units from sodium 3-(trimethylsilyl)propionate as an internal standard. The following abbreviations are used: s = singlet, d = doublet, m = multiplet and dd = double doublet. Coupling constants were evaluated by first-order rules with an estimated accuracy of 0.5 Hz. Mass spectra were recorded with a Hitachi M-80 (EI) or a JEOL JMS-DX300(FAB) spectrometer. Elemental analyses were performed with a Yanaco MT-5. Specific rotations were measured with a Horiba SEPA-200 polarimeter. Chiral HPLC analysis was performed using a YMC A-K03 (4.6 mm i.d. × 25 cm) column with 0.05 M Na$_2$HPO$_4$–H$_3$PO$_4$ (pH = 5.2)/CH$_3$CN as the eluent. This gave base-line separation of all enantiomers. All organic solvent extracts were dried over anhydrous magnesium sulfate and concentrated with a rotary evaporator under reduced pressure. Analytical data for all optically active compounds are summarized in Tables 1, 5 and 6. Racemates **3**—**8** were prepared as described in the preceding papers.[1b]

(−)-(R)-5-[(1-Methyl-1H-indol-3-yl)carbonyl]-4,5,6,7-tetrahydro-1H-benzimidazole Monohydrochloride (6R·HCl) (i) H$_2$O (1.35 l) was added dropwise to a clear solution of racemic **6** (225 g, 0.815 mol) and (+)-DIBTA hydrate (307 g, 0.816 mol) in DMF (2.7 l) at below 30 °C, followed by stirring overnight at room temperature. The resulting precipitate was collected and recrystallized three times from DMF–H$_2$O (2 : 1), using 15 volumes with respect to the amount of precipitate, to give **6R·(+)-DIBTA** (213 g, 39%) as crystals.

(ii) **6R·(+)-DIBTA** (213 g, 0.324 mol) was suspended in 1 N HCl (1.1 l), and the suspension was washed with AcOEt (3, 1, 1 l), basified to pH 9.0 with 25% aqueous NaOH (1.8 l), and extracted with CHCl$_3$–MeOH (4 : 1, 0.8 l × 2). The organic solution was dried and concentrated. The residual powder was dissolved in EtOH–AcOEt (1 : 1, 0.8 l), then 4 N HCl in AcOEt (80 ml) was added to afford a precipitate, which was collected and recrystallized from EtOH (1.1 l) to give **6R·HCl** (80.1 g, 78%) as crystals.

(−)-(S)-N-[(2-Methoxyphenyl)carbonyl]-4,5,6,7-tetrahydro-1H-benzimidazole monohydrochloride (3S·HCl), (+)-(R)-N-[(2-methoxyphenyl)carbonyl]-4,5,6,7-tetrahydro-1H-benzimidazole monohydrochloride (3R·HCl) and (+)-(S)-5-[(1-methyl-1H-indol-3-yl)carbonyl]-4,5,6,7-tetrahydro-1H-benzimidazole monohydrochloride (6S·HCl) were prepared in the same manner as above, using the appropriate (+)- or (−)-DIBTA indicated in Table 1.

(−)-(R)-5-[(1-Indolinyl)carbonyl]-4,5,6,7-tetrahydro-1H-benzimidazole Monohydrochloride (4R·HCl) (i) A mixture of racemic **4** (5.35 g, 20.0 mmol) and (+)-TA (3.00 g, 20.0 mmol) in MeOH (80 ml) was heated under reflux for 4 h, then cooled to room temperature. The resulting crystals were collected (3.48 g) and suspended in MeOH (80 ml). This suspension was heated under reflux for 4 h, then cooled to room temperature. This operation was repeated twice more to give **4R·(+)-TA** (3.02 g, 36%) as crystals.

(ii) **4R·(+)-TA** was converted to **4R·HCl** in the similar manner to that described for the preparation of **6R·HCl** (in section (ii)).

(+)-(S)-5-[(1-Indolinyl)carbonyl]-4,5,6,7-tetrahydro-1H-benzimidazole monohydrochloride (4S·HCl), (−)-(S)-4-[(4,5,6,7-tetrahydro-1H-benzimidazol-5-yl)carbonyl]-3,4-dihydro-2H-1,4-benzoxazine monohydrochloride (5S·HCl) and (+)-(R)-4-[(4,5,6,7-tetrahydro-1H-benzimidazol-5-yl)carbonyl]-3,4-dihydro-2H-1,4-benzoxazine monohydrochloride (5R·HCl) were prepared in a similar manner to that described above, using the appropriate (+)- or (−)-TA and the solvent indicated in Table 1.

(+)-(S)-5-[(1-Methyl-3-indolizinyl)carbonyl]-4,5,6,7-tetrahydro-1H-benzimidazole Monohydrochloride (7S·HCl) and (−)-(R)-5-[(1-Methyl-3-indolizinyl)carbonyl]-4,5,6,7-tetrahydro-1H-benzimidazole Monohydrochloride (7R·HCl) (i) H$_2$O (115 ml) was added dropwise to a clear solution of racemic **7** (10.0 g, 35.8 mmol) and (+)-DIBTA hydrate (13.5 g, 35.8 mmol) in DMF (175 ml). The resulting precipitate was collected as a first crop (12.0 g); the filtrate was then concentrated to a quarter volume, affording another precipitate, which was collected as the second crop (2.33 g).

(ii) The second crop (2.33 g) was recrystallized from DMF–H$_2$O (14—21 ml) to give **7S·(+)-DIBTA** (1.96 g, 7%) as crystals. **7S·(+)-DIBTA** was converted to **7S·HCl** in a similar manner to that described for the preparation of **6R·HCl** (in section (ii)).

(iii) The first crop (12.0 g) was added to 1 N HCl (120 ml), then the

solution was washed with AcOEt (60 ml × 3), basified (pH = 9) with 20% aqueous NaOH, and extracted with $CHCl_3$–MeOH (5 : 1, 60 ml × 3). The organic solution was dried and evaporated. The residual crude free base (3.12 g, 11.2 mmol) was resolved with (−)-DIBTA hydrate (4.20 g, 11.2 mmol) in DMF (73 ml), then $H_2O$ (36 ml) was added dropwise to the solution. The resulting precipitate was collected to give 7R·(−)-DIBTA (4.37 g, 16%) as crystals. 7R·(+)-DIBTA was converted to 7R·HCl in a similar manner to that described for the preparation of 6R·HCl (in section (ii)).

**(+)-(S)-5-[(3-Methyl-1-indolizinyl)carbonyl]-4,5,6,7-tetrahydro-1H-benzimidazole Monohydrochloride (8S·HCl) and (−)-(R)-5-[(3-Methyl-1-indolizinyl)carbonyl]-4,5,6,7-tetrahydro-1H-benzimidazole Monohydrochloride (8R·HCl)** (i) $H_2O$ (115 ml) was added dropwise to a clear solution of racemic 8 (10.0 g, 35.8 mmol) and (+)-DIBTA hydrate (13.5 g, 35.8 mmol) in DMF (175 ml). The resulting precipitate was collected as a first crop (9.54 g), then the filtrate was concentrated to a third volume to afford another precipitate, which was collected as the second crop (7.93 g).

(ii) The first crop (9.54 g) was recrystallized from 15 volumes of DMF–$H_2O$ (2:3). This operation was repeated twice to give 8S·(+)-DIBTA (4.63 g, 20%) as crystals. 8S·(+)-DIBTA was converted to 8S·HCl in a similar manner to that described for the preparation of 6R·HCl (in section (ii)).

(iii) The second crop (7.93 g) was recrystallized from DMF–$H_2O$ (16—32 ml) to give 8R·(−)-DIBTA (4.78 g, 18%) as crystals. 8R·(−)-DIBTA was converted to 8R·HCl in a similar manner to that described for the preparation of 6R·HCl (in the section (ii)).

**X-Ray Crystallography** Accurate unit-cell parameters for each crystal were determined using high-angle reflections. A complete set of independent reflections for each crystal was collected within the angular range of $3° < 2\theta < 120°$ in the $\theta - 2\theta$ scan mode at a scanning rate of 8° $(2\theta)$/min. Stationary background counts were recorded for 10 s before and after each scan. Three reference reflections showed no significant intensity deterioration throughout the data collection. Intensities were corrected for Lorentz and polarization factors, but not for absorption or secondary extinction.

The structures were determined with the direct methods program SHELX86[17] and were refined by block-diagonal least-squares calculation. The positions of hydrogen atoms were determined on difference Fourier electron density maps. Final refinements varied positional and anisotropic thermal parameters for non-hydrogen atoms and positional and isotropic thermal parameters for hydrogen atoms (except for some hydrogen atoms not determined on difference maps but calculated from fixed atom positions). The quantity minimized was $\sum \omega(|F_o| - |F_c|)^2$, with $\omega = 1/\sigma^2 (F_o)$. Atomic scattering factors were taken from International Tables for X-Ray Crystallography.[18]

**Molecular Modeling** Molecular modeling and conformational energy calculations were performed using the SYBYL molecular modeling software,[11] running on a Digital Equipment Corporation m-VAXII and an Evans & Sutherland PS390 graphic workstation.

**Biological Methods** Doses are expressed in terms of free base. 5-HT was purchased from E. Merck (Darmstadt, FRG) as creatinine sulfate.

**The B. J. Reflex Test[6]** Male Wistar rats weighing 200 to 250 g were anesthetized with urethane (1.25 g/kg i.p.), and the trachea was cannulated. Arterial blood pressure and heart rate were recorded on a polygraph through a pressure transducer and a cardiotachometer, respectively, connected to a catheter placed in the carotid artery. The femoral vein was also cannulated for drug injection. 5-HT at a dose of 170 nmol/kg was intravenously administered to rats at intervals of 15 min. After a stable response to 5-HT was obtained, drugs were intravenously administered to rats 10 min before 5-HT injection.

**Contraction of Isolated Guinea Pig Colon[7]** The distal portion of the colon was removed from a Hartley guinea-pig (300 to 500 g), cleaned in fresh Krebs–bicarbonate buffer at room temperature and then divided into segment of approximately 20 mm. Isomeric contraction under a loading tension of 1 g was recorded. Submaximal contraction was first elicited by repeated exposure to $10^{-6}$ M 5-HT until a constant response was obtained. Test compounds were added to the bath after the concentration–response curve for 5-HT had been obtained. The tissue was exposed to the test compound for 30 min before rechallenge with 5-HT (control). Each test compound was examined at one or two concentrations in the same preparation.

**5-HT$_3$ Receptor Binding Assay** Cell culture and membrane preparations were performed by the methods of Hoyer and Neijt[9] with minor modifications. Briefly, mouse neuroblastoma cells of the NIE-115[19] clone were grown in Dulbecco's modified Eagle's medium supplemented with 10% fetal calf serum (Gibco), penicillin (50 U/ml) and streptomycin (50 μg/ml). Cells were cultured with stirring in a humidified atmosphere containing 10% $CO_2$ at 37 °C in vessels (Corning 1000 ml, 50 rpm). When the cells had grown to a density of $2—3 \times 10^8$ cells/bottle, the culture medium was removed by centrifugation at $900 \times g$. The cell pellet was homogenized in 5 mM Tris–HCl, pH 7.4 buffer with a Polytron (setting 8.5, 2 × 10 s). The homogenate was centrifuged again at $900 \times g$. The pellet was discarded and the supernatant was centrifuged at $10000 \times g$. The membrane pellet was washed by resuspension and centrifugation in homogenizing buffer. The final pellet was resuspended to $1 \times 10^7$ cells/ml in buffer and stored at −80 °C until used for binding studies. Frozen NIE-115 cell membranes were resuspended in assay buffer. The membrane suspension, corresponding to approximately $2 \times 10^5$ cells, was incubated with [$^3$H]GR65630[8] (New England Nuclear) at 25 °C for 60 min in the dark. For competition studies a final concentration of 1.5 nM [$^3$H]GR65630 was used, while for saturation analyses six concentrations between 0.2 and 8.0 nM were used. Displacing drugs were added in a volume of 50 μl to give a final assay volume of 1.0 ml. The assays were terminated by rapid filtration under vacuum through a Whatman GF/B filter that had been presoaked in 0.1% polyethyleneimine. Filters were washed immediately four times with 4 ml of assay buffer. Radioactivity retained on the filter was determined by liquid scintillation counting. Ten μM ICS205-930 was used to define nonspecific binding in all studies. Nonspecific binding was below 10% of total binding at concentrations of [$^3$H]GR65630 that were close to the $K_d$ values.

**Cisplatin-Induced Emesis in Ferrets[14]** Male ferrets weighing 1 to 1.5 kg were used for only one experiment. Thirty minutes after i.v. injection of the test drug to the instep of a foot, cisplatin (10 mg/kg) was injected through a vein of another foot. Emesis was recorded for 4 h after injection of cisplatin and defined as rhythmic abdominal contractions, either with (vomiting) or without (retching) associated expulsion of solid or liquid material. To evaluate p.o. effects, the test drug was orally administered 1 h prior to intra-peritoneal injection of cisplatin (10 mg/kg).

**Restraint Stress Defecation in Rats[15]** Male Wistar rats weighing 180 to 320 g were used. The animals were maintained under a constant 12-h light–dark cycle. Animals were stressed by placing them in individual compartments of stress cages (Natsume Seisakusho Co., Ltd.; KN-468, W265 × L95 × H200 mm) at room temperature (23 °C). Fecal pellet output induced by restraint stress was observed using animals that had not been deprived of food before testing. A significant increase in fecal pellet output lasted for 6 h during stressing. Because the changes in fecal pellet output during the first hour after restraint were marked, the effects of the test drugs on stress-induced increases in pellet output were determined at this point. The test drugs were given p.o. 1 h or i.v. 30 min before stress.

**References and Notes**
1) a) part 1, Ohta M., Suzuki T., Koide T., Matsuhisa A., Furuya T., Miyata K., Yanagisawa I., *Chem. Pharm. Bull.*, **44**, 991—999 (1996); b) part 2, Ohta M., Suzuki T., Ohmori J., Koide T., Matsuhisa A., Furuya T., Miyata K., Yanagisawa I., *ibid.*, **44**, 999—1008 (1996).
2) a) Sanger G. J., King F. D., *Drug Design and Delivery*, **3**, 273—295 (1988); b) King F. D., Sanger G. J., *Drugs Future*, **14**, 875—889 (1989); c) Kilpatrick G. J., Bunce K. T., Tyers M. B., *Med. Res. Rev.*, **10**, 441—475 (1990).
3) Butler A., Hill J. M., Ireland S. J., Jordan C. C., Tyers M. B., *Br. J. Pharmacol.*, **94** (Suppl.), 397—412 (1988).
4) Sanger G. J., Nelson D. R., *Eur. J. Pharmacol.*, **159**, 113—124 (1989).
5) a) Schmidt A. W., Peroutka S. J., *Molecular Pharmacology*, **36**, 505—511 (1989); b) Hibert M. F., Hoffmann R., Miller R. C., Carr A. A., *J. Med. Chem.*, **33**, 1594—1600 (1990); c) Evans S. M., Galdes A., Gallm M., *Pharmacol. Biochem. Behav.*, **40**, 1033—1040

(1991).

6) Fozard J. R., Host M., *Br. J. Pharmacol.*, **77**, 520p (1982).

7) *a*) Miyata K., Kamato T., Nishida A., Ito H., Katsuyama Y., Iwai A., Yuki H., Yamano M., Tsutsumi R., Ohta M., Takeda M., Honda K., *J. Pharmacol. Exp. Ther.*, **259**, 15—21 (1991); *b*) Kamato T., Ito H., Suzuki T.,Miyata K., Honda K., *Jpn. J. Pharmacol.*, **67**, 185—194 (1995).

8) Kilpatrick G. J., Jones B. J., Tyers M. B., *Nature* (London), **330**, 746—748 (1987).

9) Hoyer D., Neijt H., *Molecular Pharmacology*, **33**, 303—309 (1988).

10) Ito H., Akuzawa S., Tsutsumi R., Kiso T., Kamato T., Nishida A., Yamano M., Miyata K., *Neuropharmacol.*, **34**, 631—637 (1995).

11) SYBYL molecular modeling software, Tripos Inc., St. Louis, MO, U.S.A.

12) Pinkus L. M., Sarbin N. S., Gordon J. C., Munso H. R. Jr., *Eur. J. Pharmacol.*, **179**, 231—235 (1990).

13) Butler A., Hill J.M., Ireland S.J., Jordan C.C., Tyers M.B., *Br. J. Pharmacol.*, **94**, 397—412 (1988).

14) Kamato T., Miyata K., Ito H., Yuki H., Yamano M., Honda K., *Jpn. J. Pharmacol.*, **57**, 387—395 (1991).

15) Miyata K., Kamato T., Nishida A., Ito H., Yuki H., Yamano M., Tsutsumi R., Katsuyama Y., Honda K., *J. Pharmacol. Exp. Ther.*, **261**, 297—303 (1992).

16) Yamano M., Kamato T., Nishida A., Ito H., Yuki H., Tsutsumi R., Honda K., Miyata K., *Jpn. J. Pharmacol.*, **65**, 241—248 (1994).

17) Sheldrick G. H., "SHELXS86. Program for Crystal Structure Solution," University of Gottingen; Federal Republic of Germany, 1986.

18) International Tables for X-Ray Crystallography, Vol. IV, Kynoch, Birmingham, 1974, pp. 71—103.

19) Kindly provided by Dr. H. Higashida, Kanazawa University, Kanazawa, Japan.